Deficiency in the anti-apoptotic protein DJ-1 promotes intestinal epithelial cell apoptosis and aggravates inflammatory bowel disease via p53

Received for publication, July 11, 2019, and in revised form, February 11, 2020 Published, Papers in Press, February 18, 2020, DOI 10.1074/jbc.RA119.010143

Jie Zhang[‡1], Min Xu[§1], Weihua Zhou[‡], Dejian Li[‡], Hong Zhang[‡], Yi Chen[‡], Longgui Ning[‡], Yuwei Zhang[‡], Sha Li[‡], Mengli Yu[‡], Yishu Chen[‡], Hang Zeng[‡], Li Cen[‡], Tianyu Zhou[‡], Xinxin Zhou[‡], Chao Lu[‡], Chaohui Yu[‡], Youming Li[‡2], Jing Sun[¶3], Xiaoni Kong[‖4], and Zhe Shen[‡5]

From the [‡]Department of Gastroenterology, The First Affiliated Hospital, School of Medicine, Zhejiang University, Hangzhou 310003, China, the [§]Department of Liver Surgery, Renji Hospital, School of Medicine, Shanghai Jiao Tong University, Shanghai 200127, China, the [¶]Department of Gastroenterology, Rui Jin Hospital, Affiliated to Shanghai Jiao Tong University School of Medicine, Shanghai 200031, China, and the [‖]Institute of Clinical Immunology, Department of Liver Diseases, ShuGuang Hospital Affiliated to Shanghai University of Chinese Traditional Medicine, Shanghai, China

Edited by Paul E. Fraser

Parkinson disease autosomal recessive, early onset 7 (PARK7 or DJ-1) is involved in multiple physiological processes and exerts anti-apoptotic effects on multiple cell types. Increased intestinal epithelial cell (IEC) apoptosis and excessive activation of the p53 signaling pathway is a hallmark of inflammatory bowel disease (IBD), which includes ulcerative colitis (UC) and Crohn's disease (CD). However, whether DJ-1 plays a role in colitis is unclear. To determine whether DJ-1 deficiency is involved in the p53 activation that results in IEC apoptosis in colitis, here we performed immunostaining, real-time PCR, and immunoblotting analyses to assess DJ-1 expression in human UC and CD samples. In the inflamed intestines of individuals with IBD, DJ-1 expression was decreased and negatively correlated with p53 expression. DJ-1 deficiency significantly aggravated colitis, evidenced by increased intestinal inflammation and exacerbated IEC apoptosis. Moreover, DJ-1 directly interacted with p53, and reduced DJ-1 levels increased p53 levels both *in vivo* and *in vitro* and were associated with decreased p53 degradation via the lysosomal pathway. We also induced experimental colitis with dextran sulfate sodium in mice and found that compared with DJ-1$^{-/-}$ mice, DJ-1$^{-/-}$p53$^{-/-}$ mice have reduced apoptosis and inflammation and increased epithelial barrier integrity. Furthermore, pharmacological inhibition of p53 relieved inflammation in the DJ-1$^{-/-}$ mice. In conclusion, reduced DJ-1 expression promotes inflammation and IEC apoptosis via p53 in colitis, suggesting that the modulation of DJ-1 expression may be a potential therapeutic strategy for managing colitis.

Inflammatory bowel disease (IBD),[6] which includes ulcerative colitis (UC) and Crohn's disease (CD), is prevalent worldwide. Evidence suggests that epithelial barrier defects play an important role in pathogenesis (1, 2). Under physiological conditions, the intestinal epithelium forms a physical and biochemical barrier between luminal bacteria and mucosal immune cells (3). To maintain intestinal barrier integrity, the number of cells produced by proliferation in the crypt bases is matched by the number of cells lost by apoptosis (4). Overactivated intestinal epithelial cell (IEC) apoptosis is frequently found in both UC and CD (5, 6, 7), leading to disruptions in intestinal barrier integrity that may allow the infiltration of bacteria from the lumen into the bowel wall (8) and trigger an inflammatory cascade, including proinflammatory cytokine production, to clear the invading bacteria (9). However, this cascade also provokes IEC death and further destroys epithelial barrier integrity, thereby creating a vicious cycle and exacerbating IBD (9–11). At present, the molecular mechanisms that regulate IEC apoptosis during the development of IBD remain elusive.

Parkinson disease (autosomal recessive, early onset) 7 (PARK7 or DJ-1) is a protein that was first reported to be associated with autosomal-recessive, early-onset parkinsonism (12, 13), and this protein is an essential regulator of a variety of cellular activities, including antioxidative activity, antiapoptotic effects (14), transcriptional regulation, chaperone activity, and protein degradation (15). DJ-1 has been shown to be an important regulator of cellular apoptosis. DJ-1 can inhibit apo-

This work was supported by National Natural Science Foundation of China Grants 81700485 (to C. L.), 81600414 (to X. Z.), and 81770547 (to J. S.). The authors declare that they have no conflicts of interest with the contents of this article.

This article contains Figs. S1–S8 and Tables S1 and S2.

[1] Both authors share co-first authorship.
[2] To whom correspondence may be addressed. Tel./Fax: 86-571-87236863; E-mail: zlym@zju.edu.cn.
[3] To whom correspondence may be addressed. E-mail: sunjingrj@shsmu.edu.cn.
[4] To whom correspondence may be addressed. Tel.: 86-212-0256188; E-mail: xiaoni-kong@126.com.
[5] To whom correspondence may be addressed. Tel./Fax: 86-571-87236863; E-mail: sz8239@zju.edu.cn.

[6] The abbreviations used are: IBD, inflammatory bowel disease; Akt, anti-apoptotic protein kinase; ASK1, apoptotic signal-regulating kinase 1; CD, Crohn's disease; CRC, colorectal cancer; DAI, disease activity index; Daxx, death domain-associated protein; DKO, double-knockout; DSS, dextran sulfate sodium; IEC, intestinal epithelial cell; IL, interleukin; PARK7, Parkinson disease (autosomal recessive, early onset) 7; TEER, transepithelial electrical resistance; TNBS, 2,4,6-trinitrobenzenesulfonic acid; TNF, tumor necrosis factor; UC, ulcerative colitis; LDH, lactate dehydrogenase; IOD, integral optical density; Gy, gray; CQ, chloroquine; IHC, immunohistochemical; CAV1, caveolin-1; Grx1, glutaredoxin; IP, immunoprecipitation; FITC, fluorescein isothiocyanate; GAPDH, glyceraldehyde-3-phosphate dehydrogenase; TUNEL, terminal deoxynucleotidyltransferase-mediated dUTP nick end labeling; PFT, pifithrin.

ptotic cell death through many downstream regulators, such as apoptotic signal-regulating kinase 1 (ASK1) (16), anti-apoptotic protein kinase (Akt) (16), death domain-associated protein (Daxx) (17), and p53 (18). Whether the antiapoptotic effects of DJ-1 play a role in maintaining intestinal barrier integrity remains unknown. Genome-wide searches have successfully identified DJ-1 as one of the susceptibility loci in IBD (19). Previous studies have suggested that DJ-1 promotes the survival of human colon cancer cells and predicts a poor prognosis in colorectal cancer (CRC) (20, 21). However, the role of DJ-1 in IBD has not been fully explored.

The tumor suppressor gene p53 is a central factor that determines cell fate and prevents the expansion of damaged and mutated cells. Many studies have shown that p53 plays a part in the development of IBD; however, the underlying mechanisms remain unclear. p53 expression is increased in colitis in both humans and mice (22, 23), positively correlated with the severity of colitis in 2,4,6-trinitrobenzenesulfonic acid (TNBS)-induced mouse models and remarkably reduced in patients treated with an anti-tumor necrosis factor (TNF) monoclonal antibody (mAb) (22). Furthermore, in p53 knockout (KO) mice ($p53^{-/-}$ mice), the apoptosis rate of IECs is significantly reduced (24). Accumulating evidence indicates that the role of DJ-1 in modulating cell apoptosis might rely on p53 expression. In a TAB-treated heart failure model, DJ-1–deficient mice were relatively prone to developing heart failure accompanied by increased cardiomyocyte apoptosis and a significantly increased p53 mRNA level (25).

In this study, we first described the down-regulated expression of DJ-1 in both CD and UC patients and mouse colitis models. Additionally, DJ-1 deficiency was found to aggravate colitis and exacerbate mucosal cell apoptosis, leading to the breakdown of the epithelial barrier. Thus, interfering with DJ-1 expression may be a potential therapeutic approach for colitis.

Results

Intestinal DJ-1 expression is reduced in IBD

To explore the role of DJ-1 in IBD, we first measured DJ-1 expression in intestinal mucosal samples from patients with active IBD and control individuals. As shown in Fig. 1*A*, DJ-1 protein expression was markedly reduced in the samples from both CD patients and UC patients compared with those from the healthy control subjects, as indicated by semiquantitative analysis of the integral optical density (IOD) of DJ-1–positive areas (Fig. 1*B*). We also found that DJ-1 protein levels were decreased in the inflamed zone compared with the noninflamed zone in individual patients (Fig. 1, *C* and *D*). Then, we examined DJ-1 levels in a mouse colitis model. Consistent with the results for the IBD patients, the DJ-1 mRNA level was decreased by ~50% in dextran sulfate sodium (DSS)-induced colitis mice (Fig. 1*E*), and DJ-1 protein expression was lower in the DSS-induced mice colon than in control mice (Fig. 1, *F* and *G*). In TNBS-induced mouse colitis models, DJ-1 had a similar expression pattern (Fig. 1*H*). IECs and bone marrow cells from wildtype (WT) mice were isolated and treated with TNFα for 6 h. A reduced DJ-1 mRNA level (Fig. 1*J*) and lower DJ-1 protein expression (Fig. 1*I*) were found in the IECs but not in the bone marrow cells (Fig. 1*L*). Reduced DJ-1 protein expression was also found in IECs from DSS-treated mice compared with those from control mice (Fig. 1*K*). Taken together, these results suggested that the down-regulation of DJ-1 expression was present in IBD.

DJ-1 deficiency aggravated DSS-induced experimental colitis

To determine the effect of DJ-1 deficiency on colitis, $DJ\text{-}1^{-/-}$ mice were generated. $DJ\text{-}1^{-/-}$ mice and control WT littermates were treated with 3.5% DSS in the drinking water for 7 days to establish an acute experimental colitis model, but the KO mice showed poor health and were sacrificed on day 6. In the KO mice, body weight began to fall on day 4 (Fig. 2*A*), which was much earlier than the time observed for the WT mice. Furthermore, higher disease activity index (DAI) scores (Fig. 2*B*) and shorter colon length (Fig. 2*C*) were observed in the KO mice than in the WT mice. Histological examination results for colon sections corresponded with the clinical observations. Compared with the WT mice, the KO mice exhibited marked disruption of the epithelial architecture, with larger areas of crypt loss, fewer goblet cells, and more severe inflammation (Fig. 2*D*), as evidenced by a significantly elevated histological score (Fig. 2*E*). The inflammatory response, especially inflammatory cytokine secretion (26), lymphocyte infiltration (27), and NF-κB signaling pathway activation (28), is an indispensable component of IBD pathogenesis. As all the mice were sacrificed on day 6 because of the poor health of the KO mice, only TNFα transcriptional levels showed a dramatic elevation after DSS treatment in colons from the WT mice. Other proinflammatory cytokines (interleukin (IL)-6 and IL-1β) and chemokines (MCP1, IL-8, and CCL3) remained unactivated, and this state was substantially exacerbated in the $DJ\text{-}1^{-/-}$ mice (Fig. 2*F*). Increased cytokine levels were also observed in the serum of the KO mice compared with that of the WT mice (Fig. S1*A*). In the colon, the neutrophil infiltration marker myeloperoxidase showed higher expression in the lamina propria of the KO mice than in that of the WT mice (Fig. S1*B*) and higher levels of the macrophage marker F4/80 were observed in the submucosa of the KO mice (Fig. S1*C*), confirming and extending the cytokine and chemokine observations. Signaling by NF-κB, which is a master regulator of gene transcription, is often dysregulated in IBD patients, resulting in overzealous inflammation (28). Furthermore, we also found that the IκBα-NF-κB signaling pathway was activated in KO mice compared with WT mice (Fig. 2*G*). We also used the Caco-2 cell line exposed to several inflammatory mediators (MIX) to establish a cell model to mimic gut inflammation in IECs (see "Experimental procedures"). Notably, knocking down DJ-1 expression with 3 small interfering RNAs (siRNAs) increased the mRNA levels of associated cytokines (TNFα and IL-8) (Fig. S1*D*). In addition, DJ-1 overexpression alleviated the expression of inflammatory mediators induced by MIX (Fig. S1*E*). Both the clinical and histological results indicated that DJ-1 deficiency markedly aggravated colitis in mice.

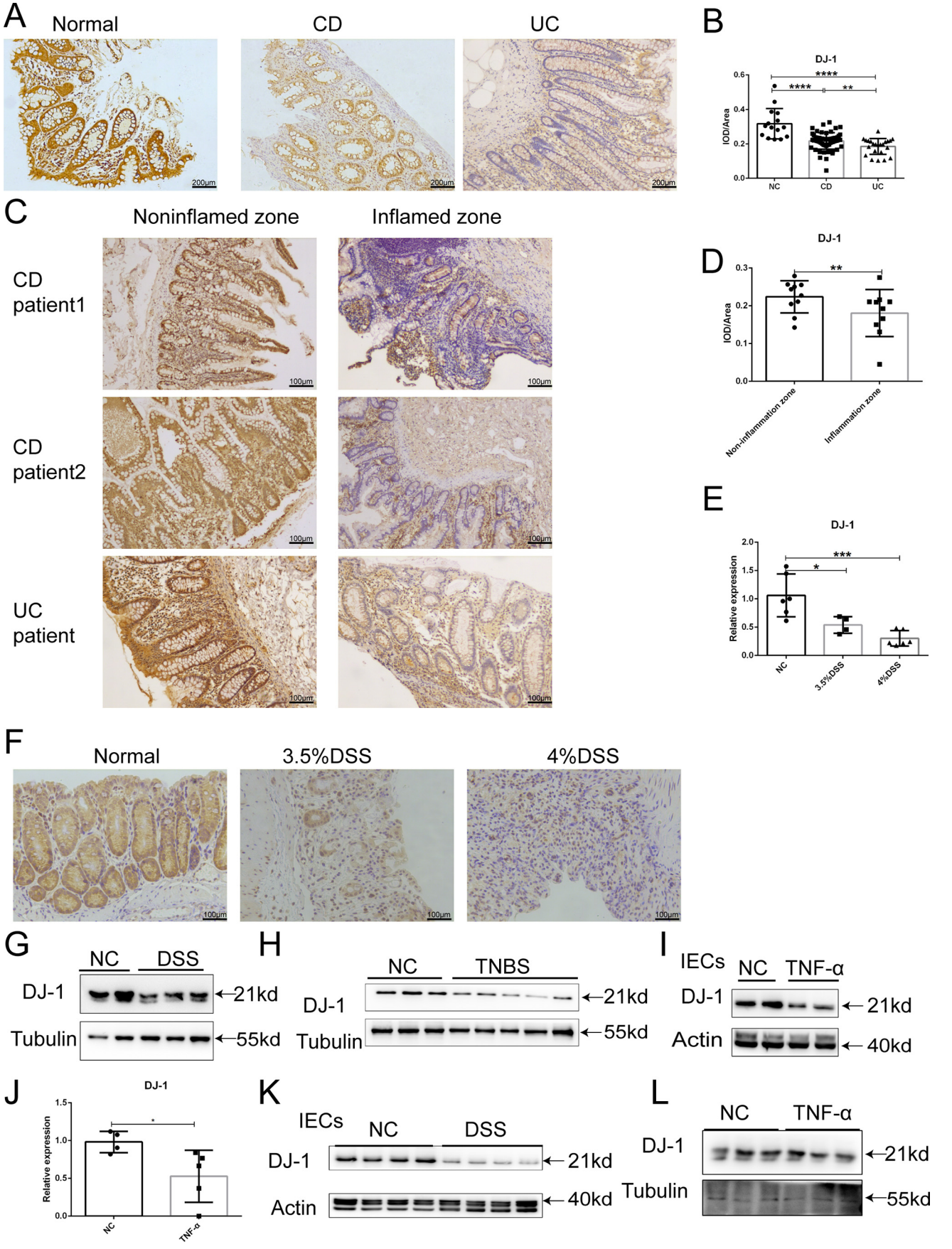
A
Normal
CD
UC
200μm
B
DJ-1
IOD/Area
NC
CD
UC
C
Noninflamed zone
Inflamed zone
CD patient1
CD patient2
UC patient
100μm
D
DJ-1
IOD/Area
Non-inflammation zone
Inflammation zone
E
DJ-1
Relative expression
NC
3.5%DSS
4%DSS
F
Normal
3.5%DSS
4%DSS
G
NC
DSS
DJ-1
21kd
Tubulin
55kd
H
NC
TNBS
DJ-1
21kd
Tubulin
55kd
I
IECs
NC
TNF-α
DJ-1
21kd
Actin
40kd
J
DJ-1
Relative expression
NC
TNF-α
K
IECs
NC
DSS
DJ-1
21kd
Actin
40kd
L
NC
TNF-α
DJ-1
21kd
Tubulin
55kd

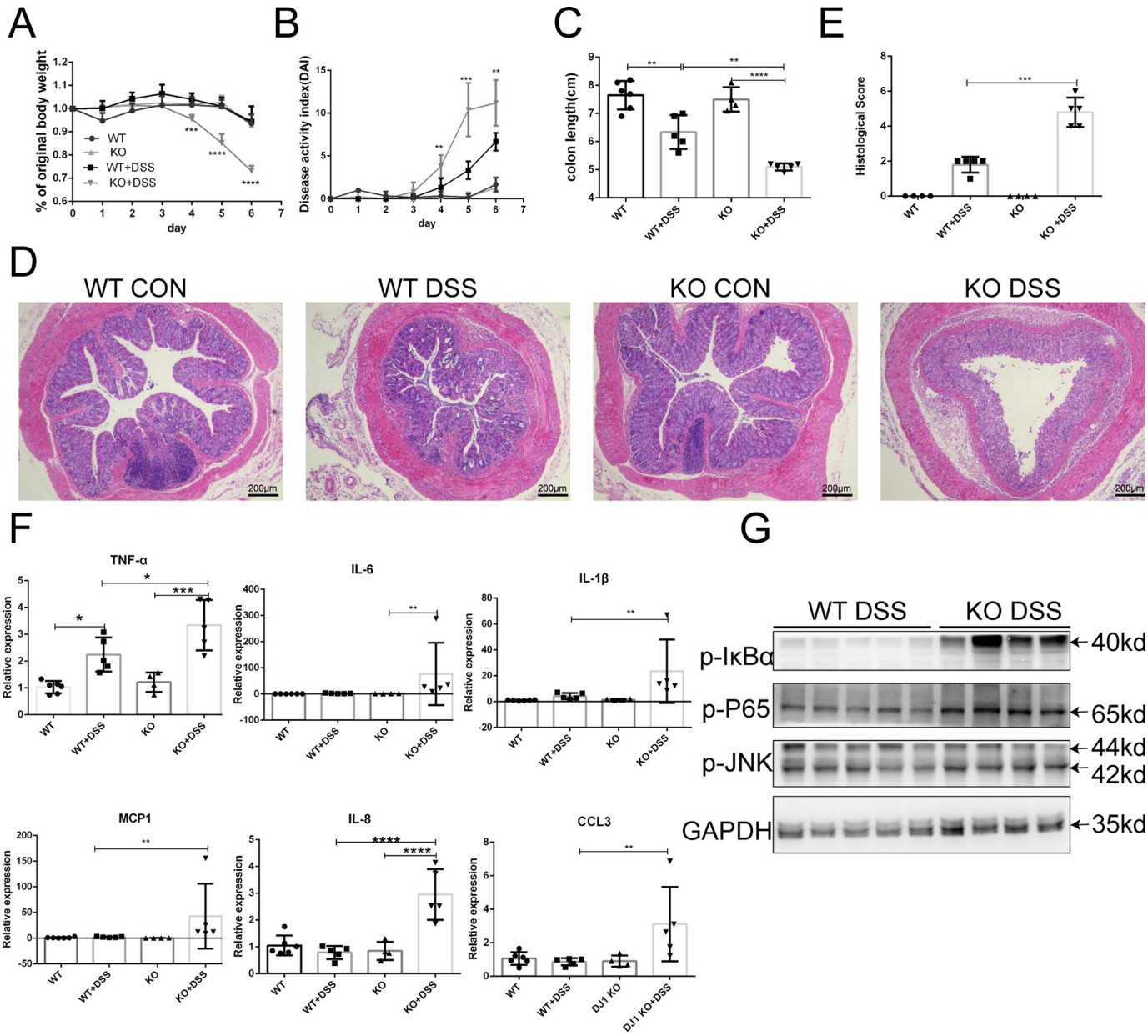

Figure 2. DJ-1 KO mice are hypersensitive to DSS-induced experimental colitis. *A–G*, WT ($n = 5$) and DJ-1 KO ($n = 5$) mice were treated with 3.5% DSS for 6 days. Body weight (*A*) and the disease activity index (*B*) calculated from weight loss, stool consistency, and bleeding were scored daily. Mice were sacrificed on day 6, and colon length (*C*) were measured. Values are expressed as the mean ± S.D. **, $p < 0.01$; ***, $p < 0.001$. *D*, histological changes in colon tissue samples from water-treated WT, water-treated DJ-1$^{-/-}$ (*KO*), DSS-treated WT (*WT DSS*), and DSS-treated DJ-1 KO (*KO DSS*) mice were examined by hematoxylin and eosin staining (original magnification, ×50). *E*, semiquantitative scoring of histopathology was then performed as described under "Experimental procedures." Values are expressed as the mean ± S.D. ***, $p < 0.001$. *F*, colons were collected from WT and KO mice after DSS treatment for cytokine and chemokine analysis. The relative mRNA levels of cytokines and chemokines in the colon were calculated. Values are expressed as the mean ± S.D. *, $p < 0.05$; **, $p < 0.01$; ***, $p < 0.001$. *G*, Western blotting was used to analyze IκBα-NF-κb protein expression in colons harvested from mice after DSS administration.

Figure 1. Reduced DJ-1 expression is found in the intestine of patients with IBD and in chemically induced mouse acute experimental colitis. *A*, Representative IHC analysis of DJ-1 expression in colonic tissue samples from healthy individuals (*Normal*), patients with UC, and patients with CD (original magnification, ×50). *B*, statistical analysis of DJ-1 expression in healthy individuals ($n = 15$), patients with UC ($n = 23$), and patients with CD ($n = 63$). Values are expressed as mean ± S.D. **, $p < 0.01$; ****, $p < 0.0001$. *C*, representative IHC analysis of DJ-1 expression in the inflamed zone and noninflamed zone of the same individual patients with IBD (original magnification, ×100). *D*, statistical analysis of DJ-1 expression in the inflamed zone and noninflamed zone in colonic tissue samples from the same patients ($n = 10$). Values are expressed as mean ± S.D. **, $p < 0.01$, paired *t* test. *E*, intestinal DJ-1 mRNA expression in normal mice ($n = 6$) and mice treated with 3% DSS ($n = 4$) or 4% DSS ($n = 6$) for 7 days was determined by quantitative PCR. Values are expressed as the mean ± S.D. *, $p < 0.05$; ***, $p < 0.001$. *F*, representative IHC analysis of DJ-1 expression in normal and DSS-treated mice (original magnification, ×100). *G*, Western blotting of DJ-1 protein expression in colon from mice treated with or without 3% DSS for 7 days. *H*, Western blotting of DJ-1 protein expression in colon from mice treated with or without TNBS. *I* and *J*, Western blotting of DJ-1 protein (*I*) and mRNA (*J*) expression in IECs treated with or without TNFα. *K*, Western blotting of DJ-1 protein expression in IECs isolated from control mice and DSS-treated mice. *L*, Western blotting of DJ-1 protein expression in bone marrow cells treated with or without TNFα.

DJ-1 expression in hematopoietic cells is essential for colitis in the DSS-induced colitis model

To determine the cell populations that contribute to the DJ-1–mediated protection against colitis, we generated 4 groups of DJ-1 bone marrow chimeras. WT and KO recipient mice received a sublethal dose of γ-ray irradiation (8.0 Gy) to kill the bone marrow cells, but all the KO recipient mice died between day 3 and 6 after irradiation, indicating that the KO mice were more susceptible to irradiation than the WT mice. Thus, a lower irradiation dose (6.5 Gy) was given to KO-recipient mice. Six weeks after bone marrow reconstitution, the genotypes of the bone marrow were evaluated (Fig. S2) and then the mice were subjected to DSS. WT to WT mice, in which DJ-1 was intact in all cells, had significantly lower body weights (Fig. S3*A*) and higher DAI scores (Fig. S3*B*) than KO to WT mice, in which DJ-1 was disrupted only in myeloid cell. Histological examination results for colon sections corresponded with the clinical observations (Fig. S3, *D* and *E*). Moreover, activation of the IκBα-NF-κB signaling pathway (Fig. 3*F*) and increased proinflammatory cytokines and chemokines (MCP1, IL-1β, CCL3, and IL-6) were observed in the WT to WT group (Fig. S3*G*), which suggested that DJ-1 in immune cells exacerbated colitis. On the other hand, the loss of body weight, DAI scores, colon shortening, histological scores, and levels of proinflammatory cytokines and chemokines in WT to KO mice in which DJ-1 was intact only in myeloid cells, were ameliorated in KO to KO mice (Fig. S3, *H–N*). Collectively, these data indicate that a lack of DJ-1 in the epithelium is critical to improve colitis, whereas the role of DJ-1 in immune cells may be the reverse.

DJ-1 deficiency contributed to IEC apoptosis

An abnormal intestinal barrier is deemed a defining feature of IBD and experimental colitis. Cell apoptosis regulation is among the diverse functions of DJ-1. On this basis, we hypothesized that DJ-1 performs a critical function in the regulation of intestinal permeability by controlling IEC apoptosis. We found that expression of Claudin1, a cell-cell adhesion molecule located at the tight junctions between cells in epithelial cell sheets (29), was barely observed in DSS-induced DJ-$1^{-/-}$ mice (Fig. S4*A*). In addition, TUNEL staining of histological sections confirmed that DJ-$1^{-/-}$ mice had greatly increased numbers of apoptotic cells in the epithelium and lamina propria of the colon, whereas WT mice showed only a mild increase in apoptotic cells (Fig. 3*A*). We also measured intestinal permeability in DJ-$1^{-/-}$ and WT mice without DSS treatment and found that the FITC-dextran level in the serum was not different between the two groups (Fig. 3*B*). However, abnormalities in epithelial permeability were much more severe in DJ-$1^{-/-}$ mice than in WT mice after DSS treatment (Fig. 3*B*). The levels of the cleaved, activated forms of caspase 3 and caspase 7 were significantly higher in DJ-$1^{-/-}$ mice than in WT mice after exposure to DSS (Fig. 3*C*). An abnormal intestinal barrier was also noted *in vitro* by using a coculture model. Transepithelial electrical resistance (TEER) increased relatively slowly in a DJ-1–silenced group transfected with a DJ-1–specific siRNA every week (Fig. S4*B*). After DJ-1 expression was knocked down in HCT116 cells for 24 h, the cells were then stimulated with human TNFα for 24 h to induce cell apoptosis. As shown in Fig. 3, *D* and *E*, the caspase 3/7 activity in the live cells and the lactate dehydrogenase (LDH) level in the culture medium were significantly elevated in the DJ-1–silenced group. Increased cell apoptosis in a DJ-1–silenced group was also found in Caco-2 cells treated with MIX (Fig. 3, *F* and *G*).

Interaction with p53 was required for DJ-1 function in IBD in vitro

The data described above suggested that the down-regulation of DJ-1 expression aggravated IEC apoptosis and barrier function lesion development in colitis. Kato and colleagues (30) found that DJ-1 bound to the DNA-binding region of p53 in a manner dependent on the oxidation of C106. Interestingly, knocking out DJ-1 significantly up-regulated colonic p53 and p21 expression in DSS-treated mice (Fig. 4*A*). Accordingly, the p53 protein level was also increased in the DJ-1–deficient HCT116 colitis model (Fig. 4*B*). Furthermore, to identify protein-protein interactions, we prepared 293T cells and HCT116 cells expressing FLAG-DJ-1 and performed co-immunoprecipitation (co-IP) assays. Our results revealed a marked interaction between DJ-1 and p53 in the two cell lines (Fig. 4, *C* and *D*). Then endogenous DJ-1 was immunoprecipitated from HCT116 cell lysates, the results showed that DJ-1 physically associated with p53 in untreated and TNFα-treated cells (Fig. 4*E*). However, how does DJ-1 alter P53 expression? The localization and phosphorylation of p53 were tested in DJ-1 knocked down cells and these cells were no different from control cells (Fig. S5*A*). DJ-1 overexpression in HCT116 cells decreased p53 expression. The cells were simultaneously treated with the proteasome inhibitor MG132 or the lysosome inhibitor chloroquine (CQ). The results showed that CQ (Fig. 4*G*) but not MG132 (Fig. 4*F*) prevented the down-regulation of p53 in the context of DJ-1 overexpression. Together, these results indicated that the degradation of p53 by DJ-1 occurred via the lysosomal pathway, accompanied by increased LC3-II and decreased p62 levels (Fig. S5*B*). p53 protein levels in both the cytoplasm and nucleus were increased after TNFα stimulation (Fig. S5*C*). An immunofluorescence staining assay showed that DJ-1 and p53 colocalized in the cytoplasm in HCT116 cells (Fig. 4*H*). Finally, we determined whether the p53 protein was implicated in human IBD. Immunohistochemical (IHC) analysis indicated that p53 expression levels were significantly higher in both CD and UC colon tissue samples than in normal control tissue samples (Fig. 4, *I* and *J*) and negatively correlated with DJ-1 expression levels in 65 paired human samples (Fig. 4*K*).

DJ-1 participated in IBD through a p53-dependent mechanism in vivo

To further test the hypothesis that p53 activation plays an essential role in mediating DSS-induced colitis in DJ-$1^{-/-}$ mice, a rescue experiment was conducted using DJ-1 and p53 double KO (DKO) mice. DKO and KO mice were treated with DSS for 7 days. Although body weight loss (Fig. 5*A*) showed no difference between the two groups, the DAI and colon length shortening were significantly ameliorated in the DKO mice compared with the KO mice (Fig. 5, *B* and *C*). Histological examination results for colon sections corresponded with the clinical observations (Fig. 5, *D* and *E*). In accordance with the

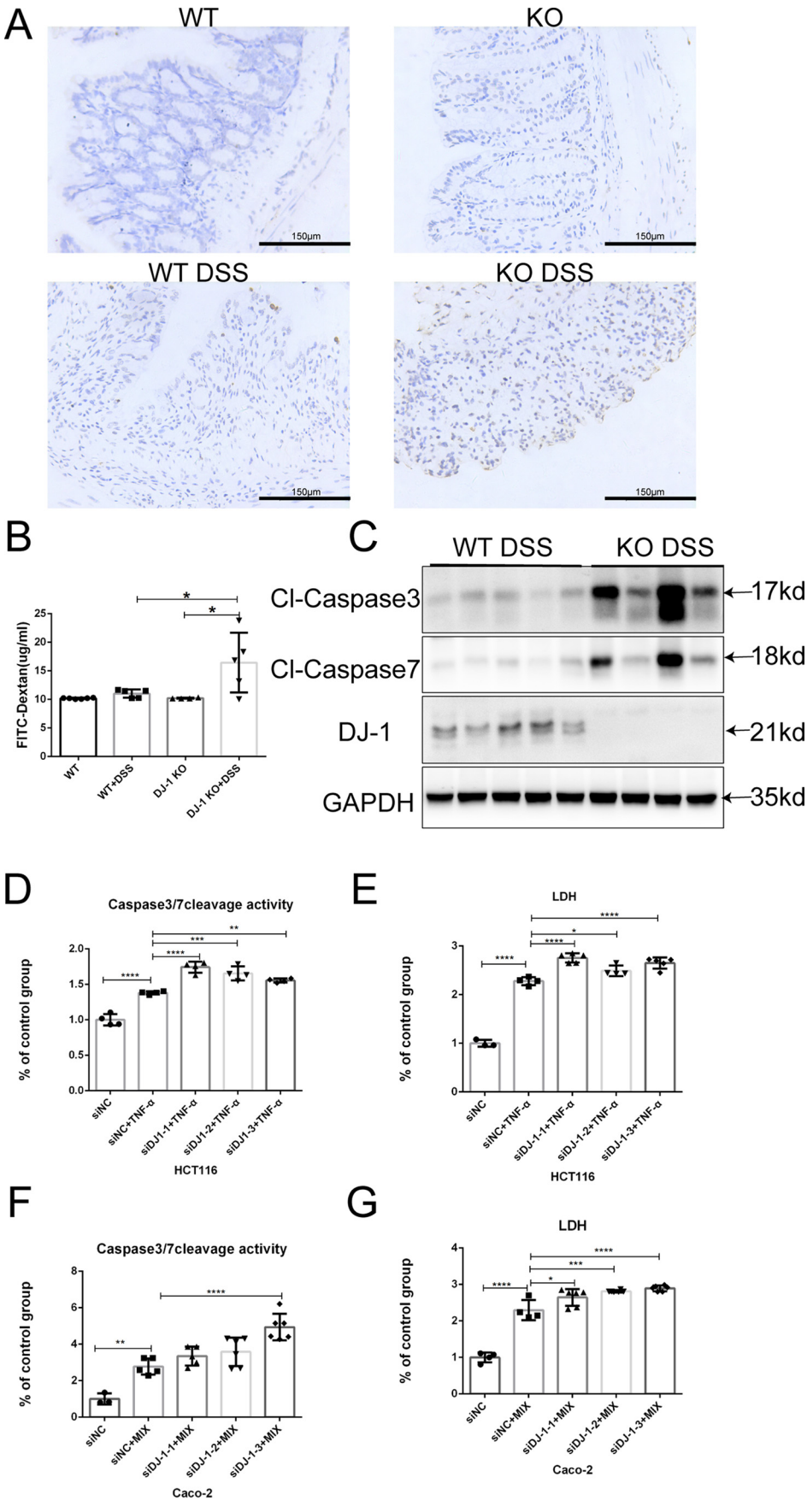
A
WT
KO
WT DSS
KO DSS
150μm
B
FITC-Dextan(ug/ml)
WT
WT+DSS
DJ-1 KO
DJ-1 KO+DSS
C
WT DSS
KO DSS
Cl-Caspase3
Cl-Caspase7
DJ-1
GAPDH
17kd
18kd
21kd
35kd
D
Caspase3/7cleavage activity
% of control group
siNC
siNC+TNF-α
siDJ-1-1+TNF-α
siDJ-1-2+TNF-α
siDJ-1-3+TNF-α
HCT116
E
LDH
% of control group
HCT116
F
Caspase3/7cleavage activity
% of control group
siNC
siNC+MIX
siDJ-1-1+MIX
siDJ-1-2+MIX
siDJ-1-3+MIX
Caco-2
G
LDH
% of control group
Caco-2

alleviated mucosal damage observed in the DKO mice, intestinal permeability was markedly decreased in these animals according to serum FITC-dextran analysis (Fig. 5*F*). The expression levels of proinflammatory cytokines and chemokines, which were prominently elevated in the KO mice, were significantly reduced in the DKO mice (Fig. 5*G*). Consistently, the DJ-1 deficiency-induced activation of caspase 3 and caspase 7 were dramatically blunted in the DKO mice (Fig. 5*H*). Furthermore, the activation of the IκBα-NF-κB signaling pathway was also decreased in the DKO mice (Fig. 5*H*). Taken together, these results suggested that the stimulatory effects of DJ-1 deficiency on the development and progression of colitis were largely dependent on p53 signaling.

Targeted suppression of p53 was an effective therapeutic strategy in DJ-1–deficient mice

We used a pharmacological inhibitor of p53 to test whether targeting p53 in DJ-1–deficient mice exerted a therapeutic effect on colitis. PFT-α was administered to both KO and WT mice by intraperitoneal injection at a dosage of 2.2 mg/kg every other day along with DSS administration. Consistently, the body weight loss and colon length shortening exacerbated by DJ-1 deficiency were observed in control KO mice, whereas these adverse effects were dramatically blunted in the KO mice intraperitoneally injected with PFT-α (Fig. 6, *A* and *B*). Histological examination results for colon sections agreed with the clinical observations (Fig. 6, *C* and *D*). The inflammatory response (Fig. 6*E*) was significantly reduced by injecting PFT-α into KO mice. The tight junction protein Claudin1 showed increased expression in the KO mice intraperitoneally injected with PFT-α compared with the KO mice injected with the vehicle (Fig. S6).

Discussion

In this study, we showed that DJ-1 played a critical role in maintaining epithelial barrier homeostasis in colitis. First, we found that intestinal DJ-1 expression was decreased in patients with UC or CD and in an acute colitis mouse model. DJ-1 deficiency increased the susceptibility of mice to DSS-induced experimental colitis. Furthermore, we found that DJ-1 deficiency promoted DSS-induced apoptosis in IECs and TNFα-induced cell apoptosis, leading to the breakdown of the epithelial barrier *in vivo* and *in vitro*, which resulted in increased susceptibility to experimental colitis. We provide the first evidence that DJ-1 performs critical functions in maintaining intestinal epithelial barrier homeostasis and thus participates in colitis.

Genome-wide association studies by genetic consortia have identified numerous variants involved in IBD pathogenesis (31). Anderson and co-workers (19) conducted a meta-analysis of 6 UC genome-wide association studies, comprising 6,687 cases and 19,718 controls, and further explored the top association signals in 9,628 cases and 12,917 controls; they found that the DJ-1 loci might be new susceptibility loci in IBD. However, the possible mechanism remains to be described. A recent study demonstrated that DJ-1 might be a novel prognostic biomarker and potential therapeutic target in human CRC (20, 21). Despite studies examining CRC, the role of DJ-1 in IBD has not been elucidated. In this study, we found that DJ-1 expression was obviously decreased in the intestine of colitis mice and in human intestinal samples from patients with CD or UC. In addition, we are the first to demonstrate that DJ-1 may be a vitally important factor in the protection against intestinal epithelium injury because completely knocking out DJ-1 increased mouse susceptibility to DSS-induced acute colitis. These findings suggested that the down-regulation of DJ-1 expression might contribute to the development of IBD.

Increased IEC apoptosis is found in both UC and CD and has been perceived to be a major homeostatic and pathogenic mechanism of IBD (32). DJ-1 deficiency can promote cell apoptosis in several disease-associated conditions. Junn and co-workers (17) proposed that DJ-1 directly interacts with Daxx, hampering the interaction between Daxx and ASK1 and thereby inhibiting ASK1 activation and cell death. DJ-1 may inhibit oxidative stress-induced apoptotic cell death not only by interacting with ASK1 directly, but also by activating and phosphorylating Akt (16). Furthermore, DJ-1 can also inhibit TRAIL-induced apoptosis by recruiting pro-caspase 8 to FADD (33). Our data first demonstrated that DJ-1 deficiency promoted DSS-induced IEC apoptosis. The FITC-dextran permeability experiment also suggested that DJ-1 could be helpful in maintaining the integrity of the colonic epithelial barrier.

After searching for potential DJ-1–interacting proteins in the STRING database, we found that p53, an inducer of epithelial cell apoptosis (22, 23, 24), was significantly activated in DJ-$1^{-/-}$ mice after DSS treatment. Several studies have demonstrated the link between p53 and DJ-1. Partly knocking down DJ-1 expression results in the up-regulation of p53 expression and increased apoptosis in the KG1 cell line. DJ-1/p53 interactions contribute to apoptosis resistance in clonal myeloid cells and may serve as a prognostic marker in patients with myelodysplastic syndrome (34). Knocking down DJ-1 expression increases Bax protein levels and accelerates the caspase 3 activation and cell death induced by UV exposure, suggesting that the cytoprotection mediated by DJ-1 involves inhibiting the p53-Bax-caspase pathway (18). These studies inspired us to determine whether DJ-1 can act as an upstream molecule of p53 for regulating apoptosis in IBD. In this study, we found that the p53 protein level was increased in DJ-1–deficient mice and that DJ-1 interacted with p53 *in vitro*. Both genetically and pharmacologically, we discovered that p53 inhibition could rescue the

Figure 3. DJ-1 restricts DSS-induced intestinal epithelial cell apoptosis. *A,* TUNEL (*brown*) staining of colonic sections from mice treated as described in the legend to Fig. 2 is shown (original magnification, ×200). *B,* these mice were fed FITC-dextran (60 mg/100 g) 4 h before sacrifice on day 6, and the serum level of FITC-dextran was detected with a microplate reader (control $n = 4–5$/group, DSS $n = 5$/group). Values are expressed as the mean ± S.D. *, $p < 0.05$. *C,* the protein levels of active caspase 3, caspase 7, and DJ-1 in the mouse colon were probed by Western blotting. *D* and *E,* DJ-1 expression was knocked down in HCT116 cells by siRNAs for 24 h, and then the cells were stimulated with 100 ng/ml of TNFα for 24 h. The activity of caspase 3/7 (*D*) and LDH (*E*) were measured as described under "Experimental procedures," and the results were normalized to control results. *F* and *G,* DJ-1 expression was knocked down in Caco-2 cells by siRNAs for 24 h, and then the cells were stimulated with MIX for 24 h. The activity of caspase 3/7 (*F*) and LDH (*G*) were measured as described under "Experimental procedures," and the results were normalized to the control results.

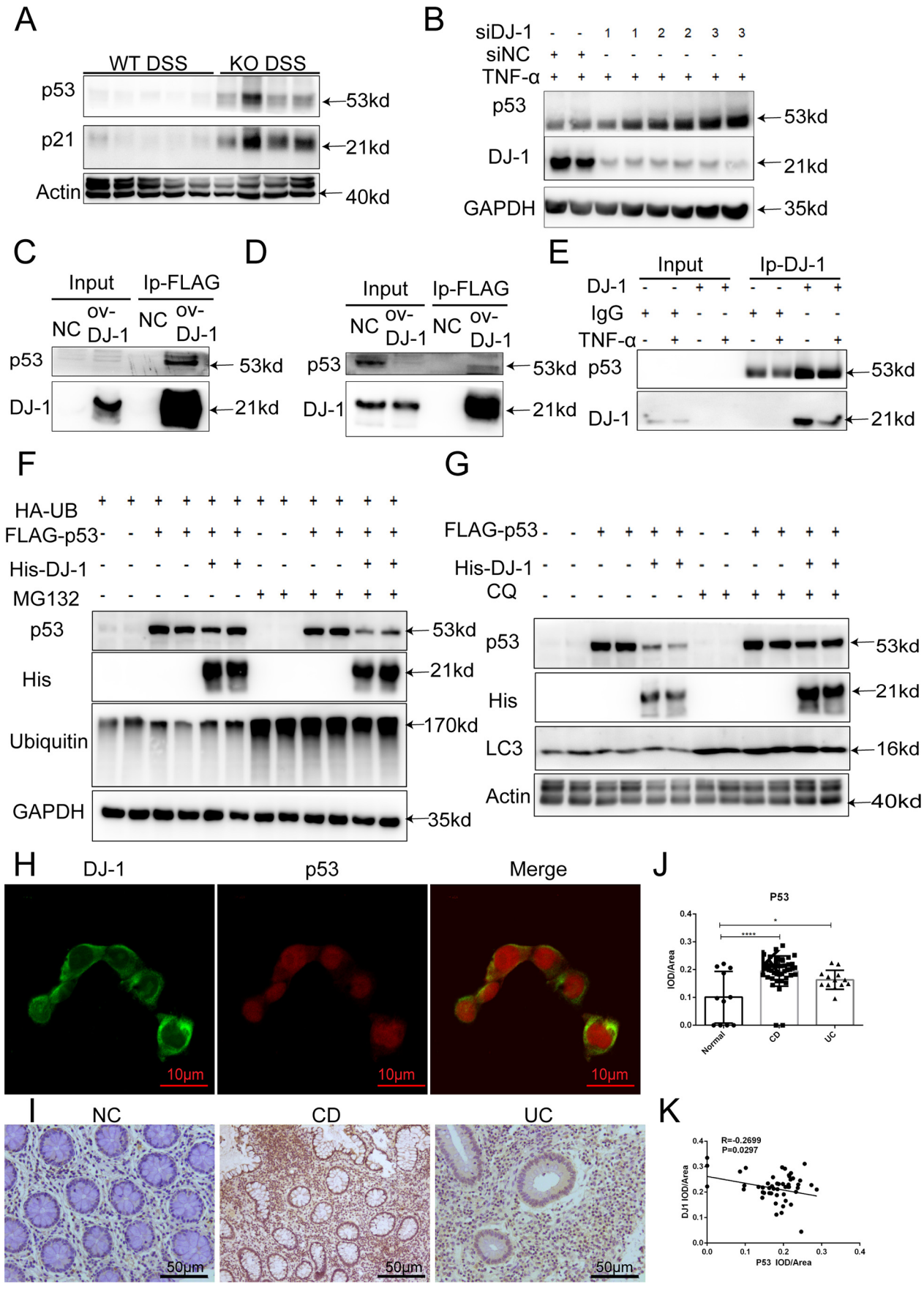
A
WT DSS
KO DSS
p53
p21
Actin
53kd
21kd
40kd
B
siDJ-1
siNC
TNF-α
p53
DJ-1
GAPDH
53kd
21kd
35kd
C
Input
Ip-FLAG
NC
ov-DJ-1
p53
DJ-1
53kd
21kd
D
Input
Ip-FLAG
NC
ov-DJ-1
p53
DJ-1
53kd
21kd
E
Input
Ip-DJ-1
DJ-1
IgG
TNF-α
p53
DJ-1
53kd
21kd
F
HA-UB
FLAG-p53
His-DJ-1
MG132
p53
His
Ubiquitin
GAPDH
53kd
21kd
170kd
35kd
G
FLAG-p53
His-DJ-1
CQ
p53
His
LC3
Actin
53kd
21kd
16kd
40kd
H
DJ-1
p53
Merge
10μm
J
P53
IOD/Area
Normal
CD
UC
K
R=-0.2699
P=0.0297
DJ1 IOD/Area
P53 IOD/Area
I
NC
CD
UC
50μm

histological damage caused by DJ-1 deficiency. In our study, we also found a pronounced negative correlation between DJ-1 expression and p53 expression in 65 paired human samples.

Based on our findings, further study is needed to clarify the mechanism leading to DJ-1 down-regulation. We found that the upstream region of DJ-1 has rarely been reported. Our group found that caveolin-1 (CAV1), a protein that aggravates colitis, might regulate DJ-1 activity. We found that the DJ-1 level was decreased in the WT mice after DSS treatment as we reported in Fig. 1, but the decreased DJ-1 was rescued in the CAV1 KO mice after DSS treatment (Fig. S7). Considering that changes in the DJ-1 level might be subjected to regulation of its upstream signal molecule, we put CAV1 as a potential upstream molecule. We are fully aware that the effect size is not as evident as we had expected; therefore further research concerning DJ-1 and caveolin-1 double KO mice is needed to identify the detailed mechanism. However, some studies have reported that DJ-1 can regulate caveolin-1 (35, 36), which is contrary to our finding, so DJ-1 and caveolin-1 double KO mice have been generated in our group. In addition, glutaredoxin (Grx1), a small thioltransferase, is considered another upstream molecule. A study reported that Grx1 could control renal tubular epithelial cell apoptosis by regulating DJ-1 (37). Knocking down Grx1 expression has also been reported to increase cell death (38) and decrease the DJ-1 protein content in different cell lines (38, 39). Overexpression of DJ-1 abolishes the cell toxicity associated with diminished Grx1 function (38). Grx1$^{-/-}$ mice have diminished levels of DJ-1 protein than WT controls (40). However, the role of Grx1 in IBD has not yet been reported, and the protein level of DJ-1 in DSS-treated Grx1 KO mice needs to be measured in future studies. Experiments regarding the role of Grx1 and DJ-1 in colitis has been undertaken. There are several limitations to our study. First, further studies are needed to determine DJ-1 mRNA levels in more CD and UC patients of different phases, such as those in mild or severe, active or remission periods. DJ-1 could probably be a monitoring indicator for severity of colitis. Additionally, evidence for reduced DJ-1 expression promoting cytotoxicity via p53 at the cellular level is lacking. siRNA or shRNA with an increased p53-silencing efficiency can be used in further studies. Mechanistically, we assumed that DJ-1 might degrade p53 through autophagy, but the underlying mechanism remains to be elucidated. Further studies are anticipated to determine the cellular mechanism of the p53–DJ-1 interaction. Furthermore, we found that DJ-1 might play different roles in different cell types. Research concerning IEC-specific DJ-1 KO mice, bone marrow-specific DJ-1 KO mice, and colonic DJ-1 overexpression awaits further exploration in future studies. In summary, our data demonstrated that a defect in DJ-1 expression might aggravate inflammation and epithelial cell apoptosis through p53 signaling in colitis, suggesting that the modulation of DJ-1 expression might be a potential therapeutic approach for colitis treatment (Fig. S8).

Experimental procedures

Tissue samples

Human paraffin-embedded colon sections from IBD patients or normal control subjects were obtained from the Department of Gastroenterology, First Affiliated Hospital, Zhejiang University, and the Department of Gastroenterology, Ruijin Hospital of Shanghai Jiaotong University. The use of colon tissue samples from patients in this study was approved by the Ethics Committee of the First Affiliated Hospital, College of Medicine, Zhejiang University, and the studies abided by the Declaration of Helsinki principles.

Mice

DJ-1$^{-/-}$ mice (The Jackson Laboratory, Bar Harbor, ME, stock number 006577, C57BL/6 background) were kindly provided by Dr. Xiaoni Kong and mated with WT mice (C57BL/6 background) to obtain mice with the DJ$^{+/-}$ genotype. p53-heterozygous KO mice (C57BL/6 background) were purchased from Biocytogen Co., Ltd. (Beijing, China). Control mice were sibling littermates obtained from crossing DJ$^{+/-}$ mice with their siblings. The genotypes of the DJ-1$^{-/-}$ mice and p53$^{+/-}$ mice were identified by using PCR as described by The Jackson Laboratory and the information provided by the company. DJ-1$^{-/-}$ mice were mated with p53$^{+/-}$ mice to generate DJ-1$^{-/-}$p53$^{-/-}$ DKO mice. Animals, which were maintained under specific pathogen-free conditions, were bred and maintained at 23 ± 2 °C on a 12-h light/12-h dark cycle at the Medical Science Institution of Zhejiang Province (Hangzhou, China). All animals were given mouse chow and water *ad libitum* (5 mice per cage). Eight- to 10-week-old male mice, weighing 20–25 g, were used for all experiments. All of the animal experiments were performed according to guidelines approved by the Animal Care and Use Committee of the First Affiliated Hospital, College of Medicine, Zhejiang University.

Induction of DSS-induced and TNBS-induced colitis and treatment

For colitis induction, mice were administered 3.5% DSS (MP Biomedicals, Solon, OH) in the drinking water for 6 or 7 days. For TNBS treatment, mice were presensitized by application of 1% TNBS (Sigma-Aldrich) to the skin for 1 week. After fasting for 24 h, the mice received 100 μl of 2.5% TNBS by rectal injection with a 1-ml syringe fitted with a catheter, as described by Wirtz *et al.* (41). For the p53 function experiment, PFT-α (Sell-

Figure 4. Interaction with p53 is required for DJ-1 function in IBD *in vitro*. *A,* p53 and p21 were analyzed by Western blotting of colonic total protein from treated mice. *B,* DJ-1 expression was knocked down by siRNAs for 24 h in HCT116 cells, the cells were stimulated with 100 ng/ml of TNFα for 24 h, and p53 expression was determined by Western blotting. *C* and *D,* HCT116 cells (*C*) or 293T cells (*D*) infected with a FLAG-tagged DJ-1 overexpression plasmid or the empty vector (*NC*) for 48 h were collected, and total FLAG-tagged DJ-1 was immunoprecipitated using M2 beads. *E,* HCT116 cell lysates were immunoprecipitated with anti–DJ-1 or control IgG antibodies. *F* and *G,* 293T cells infected with FLAG-tagged p53 and His-tagged DJ-1 were stimulated with 100 ng/ml of TNFα for 24 h and then treated with MG132 (25 μM, *F*) or CQ (50 μM, *G*) for another 4 h. *H,* representative immunofluorescence staining with a DJ-1–specific antibody (anti–DJ-1, *green*) and p53–specific antibody (anti-p53, *red*) is shown (original magnification, ×1000). *I,* representative IHC analysis of p53 expression in colonic tissue samples from healthy individuals (normal), patients with UC, and patients with CD is shown. *J,* statistical analysis of p53 expression in healthy individuals ($n = 11$), patients with UC ($n = 13$), and patients with CD ($n = 44$) was performed. The results are represented as the mean ± S.D. *, $p < 0.05$; **, $p < 0.01$; ***, $p < 0.001$, unpaired *t* test. *K,* correlative analysis of the DJ-1 IHC staining IOD/area score and p53 IHC staining IOD/area score is shown (IBD group, $n = 65$).

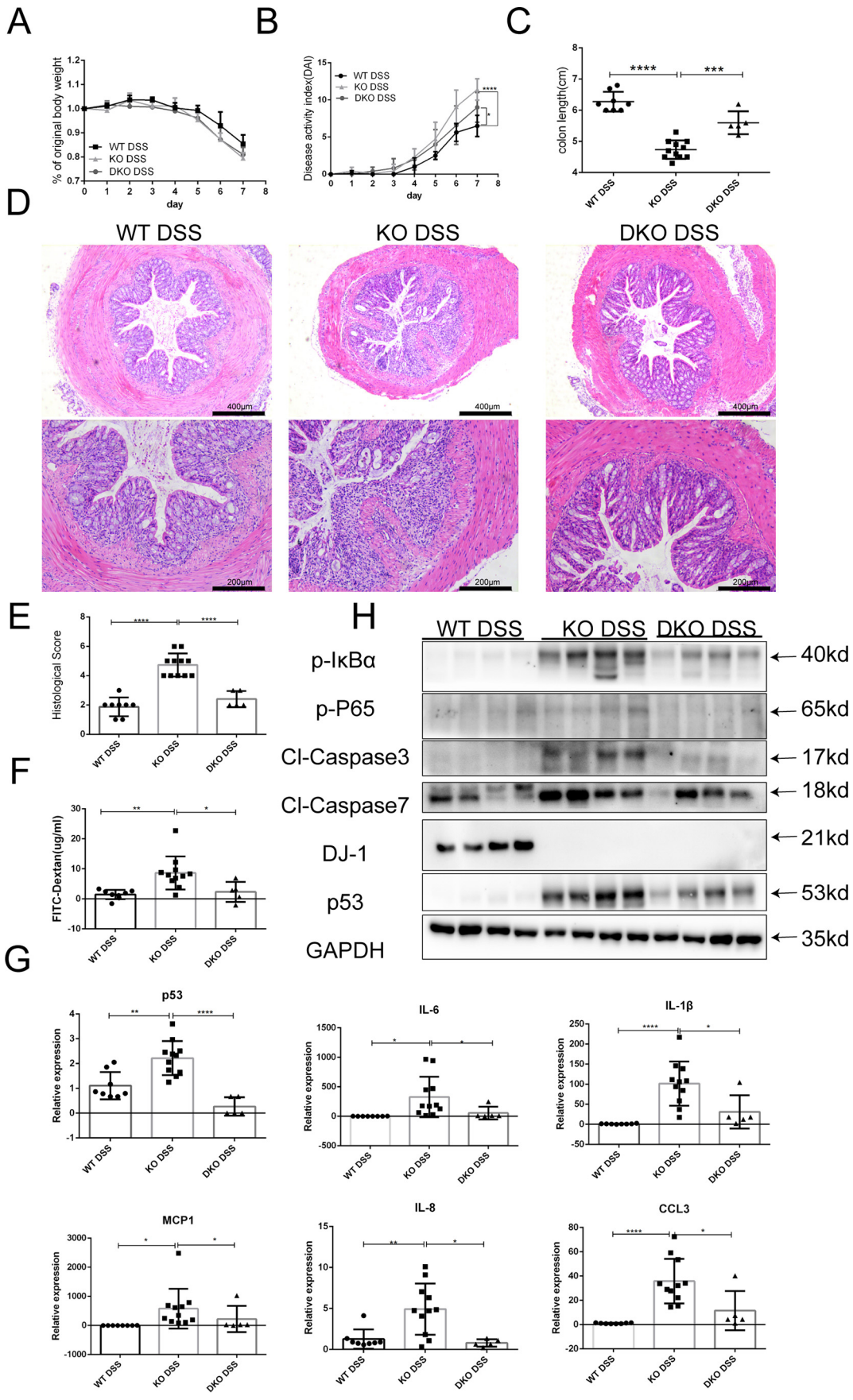
A
% of original body weight
day
WT DSS
KO DSS
DKO DSS
B
Disease activity index(DAI)
day
WT DSS
KO DSS
DKO DSS
C
colon length(cm)
WT DSS
KO DSS
DKO DSS
D
WT DSS
KO DSS
DKO DSS
400μm
200μm
E
Histological Score
WT DSS
KO DSS
DKO DSS
F
FITC-Dextan(ug/ml)
WT DSS
KO DSS
DKO DSS
G
p53
IL-6
IL-1β
MCP1
IL-8
CCL3
Relative expression
WT DSS
KO DSS
DKO DSS
H
WT DSS
KO DSS
DKO DSS
p-IκBα
p-P65
Cl-Caspase3
Cl-Caspase7
DJ-1
p53
GAPDH
40kd
65kd
17kd
18kd
21kd
53kd
35kd

eck, Houston, TX) was administered by intraperitoneal injection at a dosage of 2.2 mg/kg every other day along with DSS administration.

Determination of DAI scores

DAI scores were calculated as previously described (42). Body weight, bleeding, and stool consistency were monitored every day during colitis experiments. All scores were relative to the scores on day 0, which were set to 0. For body weight, no loss was scored as 0, 1–5% weight loss was scored as 1, 6–10% weight loss was scored as 2, 11–20% weight loss was scored as 3, and higher than 20% was scored as 4. Bleeding scores were determined as follows: 0, no blood as examined by hemoccult (Beckman Coulter) analysis, 2, positive hemoccult test, and 4, gross bleeding. For stool consistency, 0 indicated well-formed stool pellets, 2 indicated pasty and semiformed stools that did not adhere to the anus, and 4 indicated liquid stools that adhered to the anus.

Analysis of histological scores

Paraffin-embedded sections (4-mm thickness) were subjected to hematoxylin and eosin (H&E) staining for histological analysis. Histological scoring was performed as previously described (43). Briefly, scores for inflammatory cell infiltration (score 0–3) and tissue damage (score 0–3) were assessed. For inflammatory cell infiltration, the presence of occasional inflammatory cells in the lamina propria was scored as 0, the presence of increased numbers of inflammatory cells in the lamina propria was scored as 1, confluence of inflammatory cells extending into the submucosa was scored as 2, and transmural extension of the infiltrate was scored as 3. For tissue damage, no mucosal damage was scored as 0, the presence of lymphoepithelial lesions was scored as 1, the presence of surface mucosal erosion or focal ulceration was scored as 2, and extensive mucosal damage with extension into the deeper structures of the bowel wall was scored as 3. The combined histological score ranged from 0 (no changes) to 6 (extensive cell infiltration and tissue damage).

Cell culture

HCT116 cells, Caco-2 cells, 293T cells, and RAW264.7 cells were purchased from the Chinese Academy of Sciences (Shanghai, China). To develop an *in vitro* model to investigate inflammatory signaling in IECs, Caco-2 cells were exposed to the inflammatory mediators (MIX) LPS (1 μg/ml) (Sigma-Aldrich), TNFα (50 ng/ml), recombinant human interferon-γ (rhIFN-γ; 50 ng/ml), and rhIL-1β (25 ng/ml) (PeproTech, Rocky Hill, NJ) for 24 h (44). To establish a cell apoptosis model, HCT116 cells were treated for 24 h with 100 ng/ml of TNFα. Caco-2 and RAW264.7 cells were used for the co-culture system as previously described (45). HCT116 and Caco-2 cells were transfected with DJ-1–specific siRNAs (siDJ-1-1, 5′-GAUUAAGGUCACCGUUGCA-3′; siDJ-1-2, 5′-GAATTTATCTGAGTCTGCT-3′; and siDJ-1-3, 5′-TGATGAATGGAGGTCATTA-3′) or corresponding scrambled siRNAs as a negative control (forward, 5′-UUCUCCGAACGUGUCACGUdTdT-3′; reverse, 5′-ACGUGACACGUUCGGAGAAdTdT-3′) using Lipofectamine 3000 (Invitrogen). An overexpression plasmid containing the full-length DJ-1 DNA sequence or full-length p53 DNA sequence was transfected into HCT116 and HEK293T cells using Lipofectamine 3000 according to the manufacturer's instructions. Cells were transfected with siRNAs or plasmid DNA for 24 h and then incubated for another 24 h with TNFα or MIX before harvesting.

TEER measurement

TEER values were measured using a Millicell-ERS instrument (Millipore, Eschborn, Germany) according to the manufacturer's instructions.

Immunohistochemistry

Immunohistochemistry was performed as described previously (46). Five fields at a final magnification of ×100 were randomly selected for each sample, and the IOD of all the positive staining in each photograph was measured with Image Pro Plus 6.0 software.

Western blotting analysis

Western blotting analysis was performed as described previously (46). RIPA buffer (Beyotime, Jiangsu, China) was used to extract proteins supplemented with protease and phosphatase inhibitors (Invitrogen). Protein concentrations were measured using the BCA Protein Assay Kit (Beyotime). A total of 20 μg of protein from each group was separated by 12% SDS-PAGE and then electrophoretically transferred to polyvinylidene difluoride membranes (Millipore). After blocking with 5% nonfat milk (Sangon, Shanghai, China) in a Tris-buffered saline/Tween solution at room temperature for 1 h, the membranes were incubated overnight with primary antibodies at the dilutions specified by the manufacturers. The membranes were then incubated with the corresponding horseradish peroxidase-conjugated secondary antibody at a 1:5,000 dilution for 1 h. After three washes with Tris-buffered saline /Tween, specific bands were visualized using an ECL detection kit (Beyotime) and imaged with the ChemiScope 6000 Pro Touch (Clinx Science Instruments Co., Ltd., Shanghai, China). The antibodies used for this study are listed in Table S1.

Figure 5. DJ-1 participates in IBD through a p53-dependent mechanism *in vivo*. *A* and *B*, WT mice ($n = 8$), DJ-1$^{-/-}$ mice ($n = 11$), and DJ-1$^{-/-}$p53$^{-/-}$ (DKO) ($n = 5$) mice were treated with 3.5% DSS for 7 days and their body weights (*A*) and DAI scores (*B*) were monitored daily. The results are represented as the mean ± S.D. *, $p < 0.05$; ****, $p < 0.0001$. *C*, mouse colon length were measured after sacrifice. The results are represented as the mean ± S.D. ***, $p < 0.001$; ****, $p < 0.0001$. *D*, representative images of hematoxylin and eosin staining of colon tissue samples from mice are shown (original magnification, ×50 for *upper panels*; ×100 for *lower panels*). *E*, histological analysis of colon tissue samples is shown. The histological scores were determined in a double-blinded manner. The results are represented as the mean ± S.D. ***, $p < 0.001$; ****, $p < 0.0001$, unpaired *t* test. *F*, intestinal permeability was evaluated by measuring the concentration of FITC-dextran in the blood serum. *G*, quantitative RT-PCR analysis was used to assess cytokine and chemokine production in whole-colon homogenates (7 days of DSS treatment). The results are represented as the mean ± S.D. *, $p < 0.05$; **, $p < 0.01$; ***, $p < 0.001$; ****, $p < 0.0001$. *H*, immunoblotting was used to analyze cleaved caspase 3, cleaved caspase 7, and IκBα-NF-κB signaling pathway molecule protein levels in colon tissue samples from mice treated as described above. Lysates from four different mice were analyzed for each group.

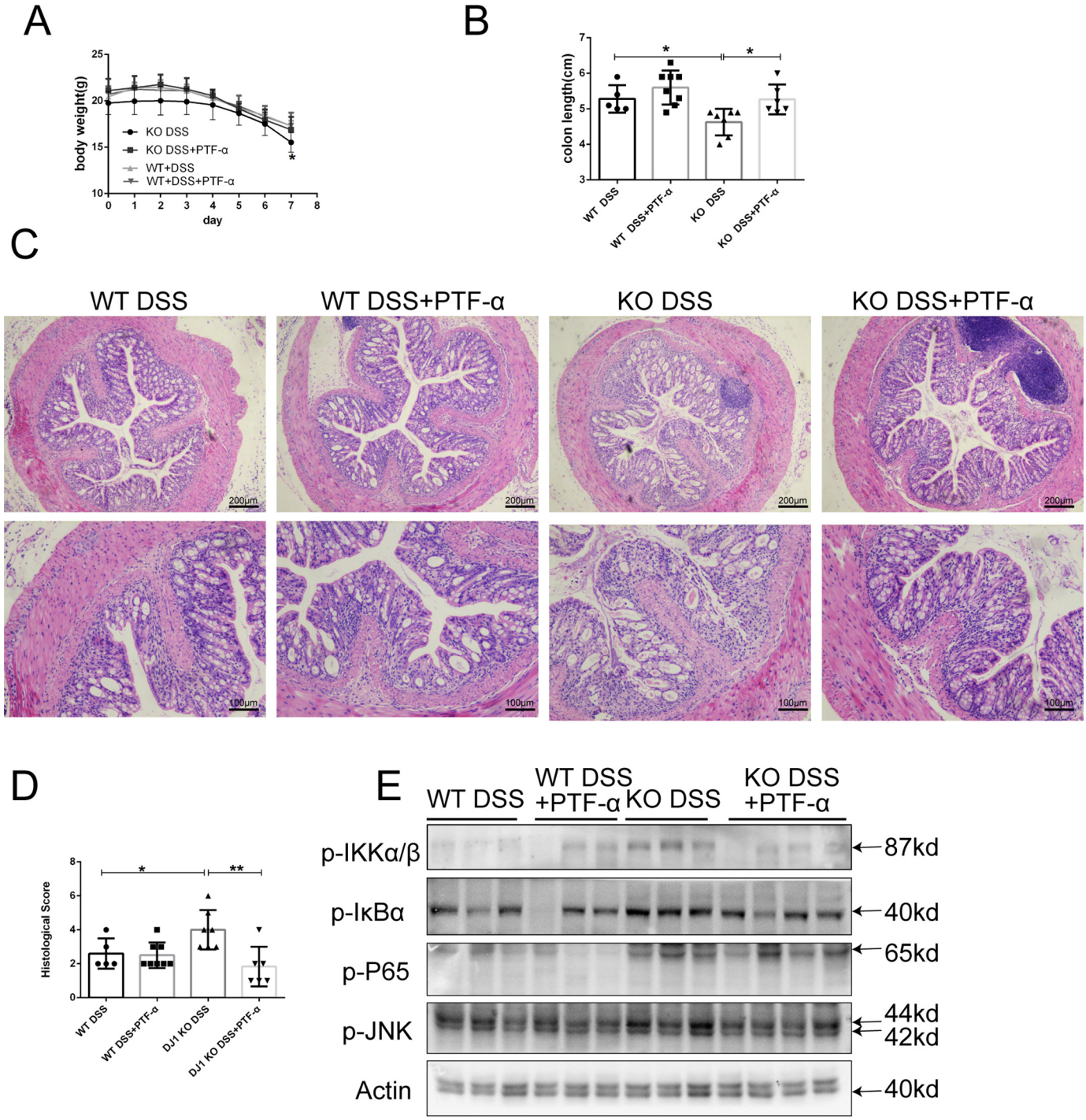

Figure 6. Targeted suppression of p53 is a therapeutic strategy for DJ-1 deficiency in mice. *A*, PFT-α was administered by intraperitoneal injection into WT mice ($n = 8$) and DJ-$1^{-/-}$ mice ($n = 6$), and the control group (WT $n = 5$, KO $n = 7$) was intraperitoneally injected with DMSO. All mice were treated with 3.5% DSS for 7 days, and their body weights were monitored daily. The results are represented as the mean ± S.D. *, $p < 0.05$. *B*, mouse colon length were measured after sacrifice. The results are represented as the mean ± S.D. *C*, representative images of hematoxylin and eosin staining of colon tissue samples from mice are shown (original magnification, ×50 for *upper panels*; ×100 for *lower panels*). *D*, histological analysis of the colon tissue samples described in *C* was performed. The histological scores were determined in a double-blinded manner. The results are represented as the mean ± S.D. *, $p < 0.05$; **, $p < 0.01$, unpaired *t* test. *E*, immunoblotting was used to analyze IκBα-NF-κB expression in colon tissue samples from mice treated as described in *A*. Lysates from three or four different mice were analyzed for each group.

Serum cytokine measurements

Serum cytokine levels were measured using the BD Cytometric Bead Array (BD Biosciences, NJ) Mouse Soluble Protein Master Buffer Kit. Briefly, mouse soluble protein standards were reconstituted and serially diluted, capture beads were mixed by design, and the standards and mouse serum samples were transferred to the appropriate assay tubes containing capture beads and incubated for 1 h at room temperature. Then, 50 μl of mixed phycoerythrin detection reagent was added to each well and incubated for 1 h. After washing,

the standards and samples were acquired on a flow cytometer.

Bone marrow chimeras

Bone marrow chimeras were established as previously reported (10). Briefly, recipient mice received a sublethal dose of γ-ray irradiation (8.0 Gy for WT mice; 6.5 Gy for KO mice) to kill the bone marrow cells, and at 6 h postirradiation, the WT and KO recipients received 100 μl of fresh WT or KO bone marrow cells at a concentration of 2×10^7/ml. Six weeks after bone marrow transplantation, blood was collected from the mice and evaluated with a DJ-1 genotyping analysis to exclude mice with failed reconstitution. Then, the mice were fed 3.5% DSS for the indicated time to induce colitis.

Immunoprecipitation

HCT116 and 293T cells were plated in 10-cm^2 dishes and then transfected with FLAG-tagged full-length DJ-1 DNA for 48 h before being lysed with 1 ml of ice-cold IP lysis buffer (Pierce) and a protease inhibitor mixture (Invitrogen). The cell lysates were immunoprecipitated with 18 μl of anti-FLAG M2 Affinity gel (Sigma) and incubated with rocking at 4 °C for 3 h (7.5 circles/min). Then, the agarose was washed four times with lysis buffer and boiled in SDS sample buffer. For endogenous protein IP, HCT116 cell lysates were immunoprecipitated using an anti–DJ-1 antibody plus protein A/G-agarose. The proteins were then separated using SDS-PAGE and subjected to Western blotting analysis with anti–DJ-1 or anti-p53 antibodies.

Analysis of apoptosis

To identify apoptotic cells in colon tissue, TUNEL staining was performed with a one-step TUNEL apoptosis assay kit (Roche, Mannheim, Germany) according to the manufacturer's instructions. To identify apoptotic cells *in vitro*, caspase-3/7 activity (Promega, Fitchburg, WI) and the LDH level (Dojindo, Kyushu, Japan) in culture supernatants were measured according to manufacturer's instructions.

Real-time PCR

Total RNA was isolated from colon tissue samples or cell lysates using the standard TRIzol (Takara, Otsu, Japan) method according to the manufacturer's instructions. The isolated RNA was reverse transcribed into cDNA using the PrimeScript® RT reagent Kit (Takara). Quantitative real-time PCR was performed using the ABI 7500 real-time PCR System (Applied Biosystems, Carlsbad, CA) with SYBR Green (Takara). The relative expression levels of target genes were normalized to the expression level of GAPDH, which was used as an internal control, and calculated by the $2^{-\Delta\Delta CT}$ method. The primer sequences are listed in Table S2.

Epithelial isolation and dissociation

IECs were isolated as previously reported (47). Briefly, colon tissue (~6 cm) from the rectum to the cecum was excised, opened, cut longitudinally, and washed in cold Dulbecco's PBS (DPBS). The intestine was first placed in ice-cold dissociation reagent number 1 and then in reagent number 2. After removing any remaining intestinal tissue, the cells were washed, dissociated with dispase, passed through 40-μm filters and used for studies.

FITC-dextran permeability assay

Intestinal permeability was assessed by oral administration of FITC-labeled dextran (M_r 4,000; Sigma-Aldrich) as previously described (9). After the withdrawal of food overnight, all mice were gavaged with FITC-dextran (60 mg/100 g of body weight) 4 h before sacrifice. The serum was then collected, and the FITC-dextran level in the serum was measured with a fluorescence spectrophotometer with emission and excitation wavelengths of 488 and 520 nm, respectively. The serum FITC-dextran concentration was calculated from standard curves generated from serial dilutions of FITC-dextran in PBS.

Statistical analysis

Statistical analysis was performed using GraphPad Prism. All data are shown as the mean ± S.D. For comparisons among three or more groups, one-way analysis of variance followed by Bonferroni analysis for multiple comparisons (for data meeting homogeneity of variance criteria) or Tamhane's T2 analysis (for data demonstrating heteroscedasticity) was performed. The differences in values between two groups were evaluated using Student's *t* test. A difference was considered statistically significant when $p < 0.05$.

Author contributions—J. Z., M. X., D. L., Yi Chen, Yishu Chen, H. Zeng, C. Y., Y. L., and Z. S. investigation; J. Z., M. X., W. Z., H. Zhang, Yi Chen, Y. Z., L. C., C. L., C. Y., and Y. L. methodology; J. Z. and Z. S. writing-original draft; H. Zhang project administration; L. N. and Yishu Chen validation; L. N., M. Y., and Z. S. visualization; S. L. software; M. Y., X. Z., and X. K. resources; L. C., T. Z., C. Y., Y. L., and Z. S. writing-review and editing; X. Z. data curation; X. Z., C. L., and J. S. funding acquisition.

Acknowledgment—We thank Professor Chenfu Xu for help with this study.

References

1. Ungaro, R., Mehandru, S., Allen, P. B., Peyrin-Biroulet, L., and Colombel, J. F. (2017) Ulcerative colitis. *Lancet* **389,** 1756–1770 CrossRef Medline
2. Mankertz, J., and Schulzke, J. D. (2007) Altered permeability in inflammatory bowel disease: pathophysiology and clinical implications. *Curr. Opin. Gastroenterol.* **23,** 379–383 CrossRef Medline
3. Peterson, L. W., and Artis, D. (2014) Intestinal epithelial cells: regulators of barrier function and immune homeostasis. *Nat. Rev. Immunol.* **14,** 141–153 CrossRef Medline
4. Hall, P. A., Coates, P. J., Ansari, B., and Hopwood, D. (1994) Regulation of cell number in the mammalian gastrointestinal tract: the importance of apoptosis. *J. Cell Sci.* **107**, 3569–3577 Medline
5. Qiu, W., Wu, B., Wang, X., Buchanan, M. E., Regueiro, M. D., Hartman, D. J., Schoen, R. E., Yu, J., and Zhang, L. (2011) PUMA-mediated intestinal epithelial apoptosis contributes to ulcerative colitis in humans and mice. *J. Clin. Investig.* **121,** 1722–1732 CrossRef Medline
6. Kiesslich, R., Duckworth, C. A., Moussata, D., Gloeckner, A., Lim, L. G., Goetz, M., Pritchard, D. M., Galle, P. R., Neurath, M. F., and Watson, A. J. (2012) Local barrier dysfunction identified by confocal laser endomicroscopy predicts relapse in inflammatory bowel disease. *Gut* **61,** 1146–1153 CrossRef Medline

7. Di Sabatino, A., Ciccocioppo, R., Luinetti, O., Ricevuti, L., Morera, R., Cifone, M. G., Solcia, E., and Corazza, G. R. (2003) Increased enterocyte apoptosis in inflamed areas of Crohn's disease. *Dis. Colon Rectum* **46,** 1498–1507 CrossRef Medline
8. Günther, C., Neumann, H., Neurath, M. F., and Becker, C. (2013) Apoptosis, necrosis and necroptosis: cell death regulation in the intestinal epithelium. *Gut* **62,** 1062–1071 CrossRef Medline
9. Liu, Y., Peng, J., Sun, T., Li, N., Zhang, L., Ren, J., Yuan, H., Kan, S., Pan, Q., Li, X., Ding, Y., Jiang, M., Cong, X., Tan, M., Ma, Y., Fu, D., Cai, S., Xiao, Y., Wang, X., and Qin, J. (2017) Epithelial EZH2 serves as an epigenetic determinant in experimental colitis by inhibiting TNFα-mediated inflammation and apoptosis. *Proc. Natl. Acad. Sci. U.S.A.* **114,** E3796–E3805 CrossRef Medline
10. Lin, W., Ma, C., Su, F., Jiang, Y., Lai, R., Zhang, T., Sun, K., Fan, L., Cai, Z., Li, Z., Huang, H., Li, J., and Wang, X. (2017) Raf kinase inhibitor protein mediates intestinal epithelial cell apoptosis and promotes IBDs in humans and mice. *Gut.* **66,** 597–610 CrossRef Medline
11. Vereecke, L., Vieira-Silva, S., Billiet, T., van Es, J. H., Mc Guire, C., Slowicka, K., Sze, M., van den Born, M., De Hertogh, G., Clevers, H., Raes, J., Rutgeerts, P., Vermeire, S., Beyaert, R., and van Loo, G. (2014) A20 controls intestinal homeostasis through cell-specific activities. *Nat. Commun.* **5,** 5103 CrossRef Medline
12. Hering, R., Strauss, K. M., Tao, X., Bauer, A., Woitalla, D., Mietz, E. M., Petrovic, S., Bauer, P., Schaible, W., Müller, T., Schöls, L., Klein, C., Berg, D., Meyer, P. T., Schulz, J. B., Wollnik, B., Tong, L., Krüger, R., and Riess, O. (2004) Novel homozygous p.E64D mutation in DJ-1 in early onset Parkinson disease (PARK7). *Hum. Mutat.* **24,** 321–329 CrossRef Medline
13. Bonifati, V., Rizzu, P., van Baren, M. J., Schaap, O., Breedveld, G. J., Krieger, E., Dekker, M. C., Squitieri, F., Ibanez, P., Joosse, M., van Dongen, J. W., Vanacore, N., van Swieten, J. C., Brice, A., Meco, G., van Duijn, C. M., Oostra, B. A., and Heutink, P. (2003) Mutations in the DJ-1 gene associated with autosomal recessive early-onset parkinsonism. *Science* **299,** 256–259 CrossRef Medline
14. Mukherjee, U. A., Ong, S. B., Ong, S. G., and Hausenloy, D. J. (2015) Parkinson's disease proteins: novel mitochondrial targets for cardioprotection. *Pharmacol. Ther.* **156,** 34–43 CrossRef Medline
15. Hijioka, M., Inden, M., Yanagisawa, D., and Kitamura, Y. (2017) DJ-1/PARK7: a new therapeutic target for neurodegenerative disorders. *Biol. Pharm. Bull.* **40,** 548–552 Medline
16. Klawitter, J., Klawitter, J., Agardi, E., Corby, K., Leibfritz, D., Lowes, B. D., Christians, U., and Seres, T. (2013) Association of DJ-1/PTEN/AKT- and ASK1/p38-mediated cell signalling with ischaemic cardiomyopathy. *Cardiovasc. Res.* **97,** 66–76 CrossRef Medline
17. Junn, E., Taniguchi, H., Jeong, B. S., Zhao, X., Ichijo, H., and Mouradian, M. M. (2005) Interaction of DJ-1 with Daxx inhibits apoptosis signal-regulating kinase 1 activity and cell death. *Proc. Natl. Acad. Sci. U.S.A.* **102,** 9691–9696 CrossRef Medline
18. Fan, J., Ren, H., Jia, N., Fei, E., Zhou, T., Jiang, P., Wu, M., and Wang, G. (2008) DJ-1 decreases Bax expression through repressing p53 transcriptional activity. *J. Biol. Chem.* **283,** 4022–4030 CrossRef Medline
19. Anderson, C. A., Boucher, G., Lees, C. W., Franke, A., D'Amato, M., Taylor, K. D., Lee, J. C., Goyette, P., Imielinski, M., Latiano, A., Lagacé, C., Scott, R., Amininejad, L., Bumpstead, S., Baidoo, L., Baldassano, R. N., *et al.* (2011) Meta-analysis identifies 29 additional ulcerative colitis risk loci, increasing the number of confirmed associations to 47. *Nat. Genet.* **43,** 246–252 CrossRef Medline
20. Zheng, H., Zhou, C., Lu, X., Liu, Q., Liu, M., Chen, G., Chen, W., Wang, S., and Qiu, Y. (2018) DJ-1 promotes survival of human colon cancer cells under hypoxia by modulating HIF-1alpha expression through the PI3K-AKT pathway. *Cancer Manag. Res.* **10,** 4615–4629 CrossRef Medline
21. Lin, Y., Chen, Q., Liu, Q. X., Zhou, D., Lu, X., Deng, X. F., Yang, H., Zheng, H., and Qiu, Y. (2018) High expression of DJ-1 promotes growth and invasion via the PTEN-AKT pathway and predicts a poor prognosis in colorectal cancer. *Cancer medicine* **7,** 809–819 CrossRef Medline
22. Spehlmann, M. E., Manthey, C. F., Dann, S. M., Hanson, E., Sandhu, S. S., Liu, L. Y., Abdelmalak, F. K., Diamanti, M. A., Retzlaff, K., Scheller, J., Rose-John, S., Greten, F. R., Wang, J. Y., and Eckmann, L. (2013) Trp53 deficiency protects against acute intestinal inflammation. *J. Immunol.* **191,** 837–847 CrossRef
23. Goretsky, T., Dirisina, R., Sinh, P., Mittal, N., Managlia, E., Williams, D. B., Posca, D., Ryu, H., Katzman, R. B., and Barrett, T. A. (2012) p53 mediates TNF-induced epithelial cell apoptosis in IBD. *Am. J. Pathol.* **181,** 1306–1315 CrossRef Medline
24. Dirisina, R., Katzman, R. B., Goretsky, T., Managlia, E., Mittal, N., Williams, D. B., Qiu, W., Yu, J., Chandel, N. S., Zhang, L., and Barrett, T. A. (2011) p53 and PUMA independently regulate apoptosis of intestinal epithelial cells in patients and mice with colitis. *Gastroenterology* **141,** 1036–1045 CrossRef Medline
25. Billia, F., Hauck, L., Grothe, D., Konecny, F., Rao, V., Kim, R. H., and Mak, T. W. (2013) Parkinson-susceptibility gene DJ-1/PARK7 protects the murine heart from oxidative damage *in vivo*. *Proc. Natl. Acad. Sci. U.S.A.* **110,** 6085–6090 CrossRef Medline
26. Sands, B. E. (2015) Biomarkers of inflammation in inflammatory bowel disease. *Gastroenterology* **149,** 1275–1285.e2 CrossRef Medline
27. Sakai, Y., and Kobayashi, M. (2015) Lymphocyte 'homing' and chronic inflammation. *Pathol. Int.* **65,** 344–354 CrossRef Medline
28. McDaniel, D. K., Eden, K., Ringel, V. M., and Allen, I. C. (2016) Emerging roles for noncanonical NF-κB signaling in the modulation of inflammatory bowel disease pathobiology. *Inflamm. Bowel Dis.* **22,** 2265–2279 CrossRef Medline
29. Tsukita, S., Tanaka, H., and Tamura, A. (2019) The claudins: from tight junctions to biological systems. *Trends Biochem. Sci.* **44,** 141–152 CrossRef Medline
30. Kato, I., Maita, H., Takahashi-Niki, K., Saito, Y., Noguchi, N., Iguchi-Ariga, S. M., and Ariga, H. (2013) Oxidized DJ-1 inhibits p53 by sequestering p53 from promoters in a DNA-binding affinity-dependent manner. *Mol. Cell. Biol.* **33,** 340–359 CrossRef Medline
31. Peters, L. A., Perrigoue, J., Mortha, A., Iuga, A., Song, W. M., Neiman, E. M., Llewellyn, S. R., Di Narzo, A., Kidd, B. A., Telesco, S. E., Zhao, Y., Stojmirovic, A., Sendecki, J., Shameer, K., Miotto, R., *et al.* (2017) A functional genomics predictive network model identifies regulators of inflammatory bowel disease. *Nat. Genet.* **49,** 1437–1449 CrossRef Medline
32. Edelblum, K. L., Yan, F., Yamaoka, T., and Polk, D. B. (2006) Regulation of apoptosis during homeostasis and disease in the intestinal epithelium. *Inflamm. Bowel Dis.* **12,** 413–424 CrossRef Medline
33. Fu, K., Ren, H., Wang, Y., Fei, E., Wang, H., and Wang, G. (2012) DJ-1 inhibits TRAIL-induced apoptosis by blocking pro-caspase-8 recruitment to FADD. *Oncogene* **31,** 1311–1322 CrossRef Medline
34. Marcondes, A. M., Li, X., Gooley, T. A., Milless, B., and Deeg, H. J. (2010) Identification of DJ-1/PARK-7 as a determinant of stroma-dependent and TNF-α-induced apoptosis in MDS using mass spectrometry and phosphopeptide analysis. *Blood* **115,** 1993–2002 CrossRef Medline
35. Gao, W., Shao, R., Zhang, X., Liu, D., Liu, Y., and Fa, X. (2017) Up-regulation of caveolin-1 by DJ-1 attenuates rat pulmonary arterial hypertension by inhibiting TGFβ/Smad signaling pathway. *Exp. Cell Res.* **361,** 192–198 CrossRef Medline
36. Kim, J. M., Cha, S. H., Choi, Y. R., Jou, I., Joe, E. H., and Park, S. M. (2016) DJ-1 deficiency impairs glutamate uptake into astrocytes via the regulation of flotillin-1 and caveolin-1 expression. *Sci. Rep.* **6,** 28823 CrossRef Medline
37. Yin, J., Xu, R., Wei, J., and Zhang, S. (2019) The protective effect of glutaredoxin 1/DJ-1/HSP70 signaling in renal tubular epithelial cells injury induced by ischemia. *Life Sci.* **223,** 88–94 CrossRef Medline
38. Saeed, U., Ray, A., Valli, R. K., Kumar, A. M., and Ravindranath, V. (2010) DJ-1 loss by glutaredoxin but not glutathione depletion triggers Daxx translocation and cell death. *Antioxid. Redox Signal.* **13,** 127–144 CrossRef Medline
39. Sabens, E. A., Distler, A. M., and Mieyal, J. J. (2010) Levodopa deactivates enzymes that regulate thiol-disulfide homeostasis and promotes neuronal cell death: implications for therapy of Parkinson's disease. *Biochemistry* **49,** 2715–2724 CrossRef Medline
40. Johnson, W. M., Golczak, M., Choe, K., Curran, P. L., Miller, O. G., Yao, C., Wang, W., Lin, J., Milkovic, N. M., Ray, A., Ravindranath, V., Zhu, X., Wilson, M. A., Wilson-Delfosse, A. L., Chen, S. G., and Mieyal, J. J. (2016)

Regulation of DJ-1 by glutaredoxin 1 *in vivo*: implications for Parkinson's disease. *Biochemistry* **55,** 4519–4532 CrossRef Medline

41. Wirtz, S., Popp, V., Kindermann, M., Gerlach, K., Weigmann, B., Fichtner-Feigl, S., and Neurath, M. F. (2017) Chemically induced mouse models of acute and chronic intestinal inflammation. *Nat. Protocols* **12,** 1295–1309 CrossRef Medline
42. Huang, L. Y., He, Q., Liang, S. J., Su, Y. X., Xiong, L. X., Wu, Q. Q., Wu, Q. Y., Tao, J., Wang, J. P., Tang, Y. B., Lv, X. F., Liu, J., Guan, Y. Y., Pang, R. P., and Zhou, J. G. (2014) ClC-3 chloride channel/antiporter defect contributes to inflammatory bowel disease in humans and mice. *Gut* **63,** 1587–1595 CrossRef Medline
43. Zaki, M. H., Boyd, K. L., Vogel, P., Kastan, M. B., Lamkanfi, M., and Kanneganti, T. D. (2010) The NLRP3 inflammasome protects against loss of epithelial integrity and mortality during experimental colitis. *Immunity* **32,** 379–391 CrossRef Medline
44. Zhu, H., Wan, X., Li, J., Han, L., Bo, X., Chen, W., Lu, C., Shen, Z., Xu, C., Chen, L., Yu, C., and Xu, G. (2015) Computational prediction and validation of BAHD1 as a novel molecule for ulcerative colitis. *Sci. Rep.* **5,** 12227 CrossRef Medline
45. Tanoue, T., Nishitani, Y., Kanazawa, K., Hashimoto, T., and Mizuno, M. (2008) In vitro model to estimate gut inflammation using co-cultured Caco-2 and RAW264.7 cells. *Biochem. Biophys. Res. Commun.* **374,** 565–569 CrossRef Medline
46. Li, M., Xu, C., Shi, J., Ding, J., Wan, X., Chen, D., Gao, J., Li, C., Zhang, J., Lin, Y., Tu, Z., Kong, X., Li, Y., and Yu, C. (2018) Fatty acids promote fatty liver disease via the dysregulation of 3-mercaptopyruvate sulfurtransferase/hydrogen sulfide pathway. *Gut* **67,** 2169–2180 CrossRef Medline
47. Gracz, A. D., Puthoff, B. J., and Magness, S. T. (2012) Identification, isolation, and culture of intestinal epithelial stem cells from murine intestine. *Methods Mol. Biol.* **879,** 89–107 CrossRef Medline